



## Hybrid design of optimal shunt capacitor allocation and reconfiguration of radial distribution systems considering techno-economic benefits

Ifeoluwa Olajide Fajinmi<sup>a</sup>, Gafari Abiola Adepoju<sup>a</sup>, Sunday Adeleke Salimon<sup>b,\*</sup>,  
Kareem M. AboRas<sup>c</sup>, Oluwaseyi Wasiu Adebisi<sup>a</sup>, Olubunmi Onatoyinbo<sup>b</sup>,  
Mohammad Khishe<sup>d,e,f,\*</sup> , Pradeep Jangir<sup>g,h,i</sup>, Wulfran Fendzi Mbasso<sup>j,k,\*</sup> 

<sup>a</sup> Electronic and Electrical Engineering Department, Ladoko Akintola University of Technology, Ogbomosho, 210214, Oyo State, Nigeria

<sup>b</sup> Electrical and Electronic Engineering Department, Redeemer's University, Ede 232101, Osun, Nigeria

<sup>c</sup> Department of Electrical Power and Machines, Faculty of Engineering, Alexandria University, Alexandria 21544, Egypt

<sup>d</sup> Department of Electrical Engineering, Imam Khomeini Naval Science University of Nowshahr, Nowshahr, Iran

<sup>e</sup> Applied Science Research Center, Applied Science Private University, Amman, Jordan

<sup>f</sup> Jadara University Research Center, Jadara University, Irbid, Jordan

<sup>g</sup> Centre for Research Impact & Outcome, Chitkara University Institute of Engineering and Technology, Chitkara University, Rajpura, 140401, Punjab, India

<sup>h</sup> Adjunct Professor, Department of CSE, Graphic Era Hill University, Dehradun, 248002, India

<sup>i</sup> University Centre for Research and Development, Chandigarh University, Gharuan, Mohali 140413, India

<sup>j</sup> Department of Biosciences, Saveetha School of Engineering, Saveetha Institute of Medical and Technical Sciences, Chennai 602 105, India

<sup>k</sup> Technology and Applied Sciences Laboratory, U.I.T. of Douala, P.O. Box 8689 Douala, University of Douala, Cameroon

### ARTICLE INFO

#### Keywords:

Radial distribution networks  
Reconfiguration  
Shunt capacitors  
Cost benefits  
Dandelion optimizer

### ABSTRACT

Efficient power delivery is crucial for power distribution systems, prompting utilities to consistently seek out new technologies to improve their performance. Managing power loss and cost efficacy stands out as a critical concern, directly impacting systems efficiency. Hence, this study provides an innovative method for the performance enhancement of radial distribution networks (RDNs) through simultaneous reconfiguration and Shunt Capacitor (SC) allotment utilizing a newly developed Dandelion Optimizer (DO) and a novel objective function. The main aim of the optimization process is to maximize economic benefits while also assessing technical advantages. Technical benefits include real power loss, Average Voltage Stability Index (AVSI), and Voltage Profile Index (VPI), while economic benefits involve evaluating cost reductions due to decreased power purchased and losses, as well as the SC and switching costs spanning a 20-year planning period. Tests were conducted on IEEE 33- and 69-bus RDNs using the suggested methodology under various scenarios, including reconfiguration, SC integration, and synchronous reconfiguration with SC allocation, and the model was simulated using MATLAB software. The optimal solution was achieved by simultaneously reconfiguring and allocating SCs to maximize total cost benefits. For the 33-bus system, this resulted in power loss, AVSI, VPI, and total cost-benefit values of 82.84 kW (62.90 % reduction), 0.9566 p.u., 1.9190 p.u., and \$ 773 752.85, respectively, while for the 69-bus system, the corresponding values were 43.8 kW (80.51 % reduction), 0.9874 p.u., 2.4680 p.u., and \$ 1.1347 million. Comparing the technique with other methods, its effectiveness was established, and it was shown to perform better with power loss reduction chosen as assessment metric.

### 1. Introduction

Efficient power distribution remains a central focus for electrical engineers, researchers, and technological innovators alike. Key to this

efficiency is the reduction of losses within the distribution system, encompassing various elements such as conductors, transformers, and feeders [1]. The distribution network acts as the crucial interface between end-users and the broader grid infrastructure [2,3]. Typically configured as radial or weakly meshed structures, these networks enable

\* Corresponding authors.

E-mail addresses: [fajinmiifeoluwa123@gmail.com](mailto:fajinmiifeoluwa123@gmail.com) (I.O. Fajinmi), [gaadeoju@lautech.edu.ng](mailto:gaadeoju@lautech.edu.ng) (G.A. Adepoju), [salimonsun@run.edu.ng](mailto:salimonsun@run.edu.ng) (S.A. Salimon), [kareem.aboras@alexu.edu.eg](mailto:kareem.aboras@alexu.edu.eg) (K.M. AboRas), [adebiyiseyi2@gmail.com](mailto:adebiyiseyi2@gmail.com) (O.W. Adebisi), [onatoyinboo@run.edu.ng](mailto:onatoyinboo@run.edu.ng) (O. Onatoyinbo), [m\\_khishe@alumni.iust.ac.ir](mailto:m_khishe@alumni.iust.ac.ir) (M. Khishe), [pkjmtch@gmail.com](mailto:pkjmtch@gmail.com) (P. Jangir), [fendzi.wulfran@yahoo.fr](mailto:fendzi.wulfran@yahoo.fr) (W.F. Mbasso).

<https://doi.org/10.1016/j.rineng.2025.104385>

Received 30 October 2024; Received in revised form 11 January 2025; Accepted 17 February 2025

Available online 18 February 2025

2590-1230/© 2025 The Author(s). Published by Elsevier B.V. This is an open access article under the CC BY license (<http://creativecommons.org/licenses/by/4.0/>).

Nomenclature		<i>IntR</i>	Interest rate
<i>Parameters</i>		<i>Abbreviations</i>	
$SC_{MC}$	Shunt capacitor maintenance cost	DO	Dandelion Optimizer
$SC_{inv\_cost}$	Shunt capacitor investment cost	RDN	radial distribution network
$S_{inv,s}^{Cost}$	Switch investment cost	NR	Network reconfiguration
$S_{O\&M,S}^{Cost}$	Switch maintenance and operation cost	SCA	Shunt capacitor allocation
$C_{Grid}$	Cost of grid-supplied electricity	DG	Distributed generation
$CB_p$	Cost-benefit from the decreased price of electricity purchased	VPI	Voltage profile index
$V_i$	Voltage at bus $i$	AVSI	Average voltage stability index
$I_i$	Current flow via distribution line	MBA	Modified bat algorithm
$V_\beta$	Average bus voltage	ICSA	Improved cuckoo search algorithm
$V_\chi$	Standard deviation of the bus voltages	HSA	Harmony search algorithm
$G_{ij}$	Conductance between node $i$ and $j$	FWA	Fireworks algorithm
$B_{ij}$	Susceptance between node $i$ and $j$	ACSA	Ant colony search algorithm
$P_{gi}$	Real power generated at bus $i$	HM	Heuristic Method
$P_{Di}$	Real power demanded at bus $i$	\$/npy	Dollars per number of planning years
$Q_{gi}$	Reactive power generated at bus $i$	UVDA	Uniform voltage distribution based constructive algorithm
$Q_{Di}$	Reactive power demanded at bus $i$	INNA	Improved neural network algorithm
$LB$	Lower bound	ACA	Ant colony algorithm
$UB$	Upper bound	SFS	Stochastic fractal search
$X_{elite}$	dandelion seed propagation's best location	GWO	Grey wolf Optimizer
$f_{best}$	Best fitness score	AWOA	Adaptive whale optimization algorithm
$Dim$	variable dimension	LS	Least square optimizer
$pop$	population size	MLIP	Mixed linear integer programming
$\beta$	Local adaptive parameter	BFO	Bacterial foraging algorithm
$randn$	Arbitrary number after standard normal distribution	MBBO	Modified biogeography-based optimization
$X_{mean,t}$	Average location of the dandelions in $ith$ iteration	CS	Cuckoo search algorithm
$\beta_t$	Brownian motion	MIC	Modified imperialist competitive algorithm
$InfR$	Inflation rate	APSO	Adaptive particle swarm optimizer

the unidirectional flow of power from substations to different nodes. Referred to as radial distribution networks (RDNs), they are preferred for their simplicity in operation, cost-effectiveness, and ease of maintenance and protection [4]. However, RDNs face notable challenges, particularly concerning significant power losses and voltage fluctuations along their distribution paths [5]. These issues manifest due to the network's inherent high resistance to reactance ratio and the prevalence of heavy inductive loads [6] like transformers, AC induction motors, and adjustable speed drives (ASDs) [4,7]. Research indicates that distribution networks incur substantial losses, with approximately 13% of the total generated power dissipated within these systems. Furthermore, distribution systems are responsible for approximately 70% of all losses within the broader electrical power system [8]. Consequently, ongoing efforts are directed towards addressing these challenges by tackling bus voltage fluctuations and minimizing power losses. Such endeavors are critical to enhancing the distribution networks' overall reliability and performance in meeting the growing demands of modern energy distribution [9,10].

Feeder reconfiguration is an act of altering a DN's topology by modifying the switches' positions. Two types of these switches exist in the DNs: normally closed (N.C.) and normally open (N.O.). Within the network, N.O. switches serve as tie switches. [11]. During reconfiguration, their statuses are optimized based on predefined objective functions. The amount of losses in the DN can be efficiently influenced by changing the statuses of these switches [12]. Parallel to this, capacitors are essential to distribution networks' reactive power correction [13, 14]. They are also employed to lessen energy losses and enhance voltage profiles [15]. The efficacy of capacitor-based compensation hinges on its strategic placement within the network. Recent research has explored the synergistic benefits of simultaneously employing optimal allotment

of capacitors and reconfiguration of distribution networks to decrease energy losses using different objective functions over time [16]. Nonetheless, the efforts to continually optimize the performance of DNs by integrating various objective functions through combined methodologies should not be relaxed.

The cultural algorithm (CA) and the cuckoo search algorithm (CSA) for the optimal NR and integration of SCs in a smart distribution system were introduced in Ref. [17]. The optimization process's chosen objective function was real power loss, with the primary goals being losses diminution and the improvement of voltage profiles. In [9], an adaptive particle swarm optimization (APSO) method was proposed with the goal of decreasing power losses for synchronous reconfiguration and shunt capacitor placement in RDNs. Using the IEEE 33-bus and the Nigerian Ayepe 34-bus RDNs as test beds, the effectiveness of the selected APSO was shown. Using the DGs hosting capacities (HC) and real power loss as objective functions, the authors in [18] presented the SHADE optimization algorithm and the switch opening and exchange (SOE) method for solving a multi-objective optimization NR (network reconfiguration) and optimal placements of renewable-based DGs and SC in RDNs. The multi-objective NR and SC unit allotment in RDNs presented a by [19] made use of an improved artificial bee colony optimization (EABCO) approach. The function of the optimization was for the voltage deviation index (VDI) and active power losses diminution. In [20], different loading conditions were taken into consideration for a multi-objective NR and the allotment of capacitor banks in RDNs using a modified particle swarm optimization (MPSO). The optimization's objective functions were diminution of cumulative voltage deviation and the loss of active and reactive power. For the purpose of allocating DGs and SCs in a reconfigured RDN, Biswal et al. in [21] proposed the Quasi-reflected slime mold method (QRSMA). The optimization procedure made use of a

multi-objective function that minimized the system's expenses, reduced its overall real power loss, reduced its cumulative voltage deviation index, and increased its reliability indices.

Additionally, for simultaneous reconfiguration and SCs in RDNs, the authors in [22] suggested a mixed-integer linear programming (MLIP) model aiming to reduce active power loss. For a probabilistic multi-objective NR and optimal allotment of SCs and DG in DNs, Ref. [23] described the use of a multi-criteria decision-making (MCDM) algorithm. The objective function of this algorithm was aimed at real power losses and voltage deviation index diminution while simultaneously maximizing loading margins. Artificial ecosystem optimizers (AEOs) were also used in [24] to optimize the NR and allotment of SCs and DGs in DNs, with the objective of reducing active power losses. The objective of [25] was aimed at real power loss and the operating costs diminution by applying Johnson's algorithm and the adaptive whole optimization (AWO) algorithm for synchronous NR and SC allotment in RDNs. The objective of [26]'s NR and SCA systems was to minimize real power loss by applying the moth swarm algorithm (MSA). To reduce the yearly energy losses of balanced and unbalanced DNs, system reconfiguration and the best possible distribution of shunt capacitor banks were implemented in [27] using the modified Tabu search and the Harper sphere search algorithms (MTS-HSSA). The objective function used in Ref. [28] presented the grey wolf optimizer for the optimal RDNR and integration of SCs and DGs for power loss minimization. The objective function of the discrete improved grey wolf optimizer (DIGWO), which was used for NR and SCA, was to minimize the annual operating cost [29]. For the purpose of NR and SC allotment in DNs, the authors in reference [30] employed a hybrid simulated annealing-minimum spanning tree approach. In [31], reconfiguration, distributed energy resources (DERs), and SC integration in distribution networks were achieved by using the Boolean algebra and particle swarm optimization (PSO) in binary space, with the objective function being minimized active power losses and maximized VSI. A stochastic model was applied in Ref. [32] to reflect the influence of unpredictable loads on distribution network reconfiguration. Minimizing the active power losses in the networks was the objective of the obtained objective function. Reconfiguration of DNs to improve dependability and reduce active power losses through application of the particle swarm optimization (PSO) and genetic algorithms was introduced in [33]. With the goal of minimizing aggregated voltage deviation index, maximizing VSI, and minimizing power losses, the authors of [34] introduced a multi-objective Teaching Learning based optimizer (TLBO) for reconfiguring and integrating DG and SC units on balanced and unbalanced networks [35].

The literature reviewed on simultaneous reconfiguration and capacitor placement considered various objective functions ranging from technical parameters like power loss, voltage deviation, and voltage stability. Most works did not consider the technical and economic benefits of this approach. Some literature, such as [25], that even considered economic benefits only focused on evaluating the reduced operating costs. They never factored in the process's switching costs and the cost per reactive compensation. Moreover, they focused only on the assessment for a single year, not considering the impact of inflation and interest rates. In the technological and economic world, profits or benefits obtained from devices cannot be the same throughout the lifespan of the device or machine due to depreciation, inflation, and interest rates accounting for the reduction of the lifespan of the device and instability of market prices over time. Hence, the economic benefits may not be accurately accounted for without considering the effect of inflation and interest rates. Taking note, this research proposes a unique techno-economic benefit approach over several years of planning, considering the effect of inflation and interest rates for optimal NR and integration of shunt capacitors in RDNs. Additionally, a summary of the results from the reviewed literature showed that maximum active power loss reduction for those that implemented their approach on the IEEE 33-bus distribution system, ranged from 42.68–58.82 %, likewise, for the IEEE 69-bus distribution system, the maximum active power loss

reduction ranged from 54.28–69.37 %, except in [17] that reported 76.95 % reduction. While the results are impressive, there can still be improvement in the loss reduction obtained in these distribution systems. Hence, in addition to enhancing the cost efficacy of RDNs, this approach aims to achieve improved loss reduction compared to previous techniques.

A novel dandelion optimizer (DO) is proposed to be applied for the simultaneous reconfiguration and SC unit allocations in RDNs, considering maximizing the total cost benefits under various scenarios of a single and mixed combination of the two loss reduction techniques (NR and SCA). The technical and economic advantages of the changes produced by the NR and allotment of the SC units in the RDNs are to be evaluated. The active power loss diminution, the Voltage Profile Index (VPI), and the Average Voltage Stability Index (AVSI) are the technical parameters evaluated. The economic benefits is achieved by analysing the cost-benefit of purchasing less power due to a matching decrease in power loss after accounting for the expenses of the SC and switching over a 20-year planning period. Thus, the manuscript contributes to the field by offering a more holistic optimization approach that aligns technical efficiency with economic viability, setting a new benchmark for future research in power distribution optimization.

The following highlights this study's major contributions:

- A novel algorithm for SC allotment and reconfiguration in distribution networks.
- A novel objective function for maximizing cost benefits through NR and SC allotment.
- For the first time, VPI is assessed concerning reconfiguration and SC allocation.
- Improved power loss reduction for NR and SCA compared to existing methods.

The remaining sections of the paper are structured as follows: [Section 2](#) discusses the mathematical derivation of the objective function utilized for optimization, the mathematical expressions of all the technical benefits assessed, and the constraints to which the optimization was subjected. [Section 3](#) presents the overview of the optimization technique (DO) used and its application for NR and SCA. [Section 4](#) discusses the result of simulations for all scenarios considered, including an objective comparison of the proposed approach with existing techniques. [Section 5](#) presents a summary of the discussions presented throughout the article and directions for future research.

## 2. Problem formulation

The proposed work's objective function and the various restrictions imposed on the optimization procedure are explained in this section.

### 1. Objective function

The goal selected for this research is to maximize the overall cost benefits from SC deployment in conjunction with RDN reconfiguration. The objective function's mathematical model is expressed as follows:

#### A. Capacitor installation cost

The annual maintenance cost ( $SC_{MC}$ ) plus the SC investment cost ( $SC_{inv\_cost}$ ) make up the total shunt capacitor cost ( $SC_{COST}$ ).

$$SC_{COST} = SC_{inv\_cost} + SC_{MC} \quad (1)$$

$$SC_{inv\_cost} = \sum_{i=1}^{n_{cap}} Q_{cap,i} \times IC_{cap} \quad (2)$$

$$SC_{MC} = MC_{cap} \times \sum_{y=1}^{N_{yrs}} \left( \frac{1 + \text{inf}R}{1 + \text{int}R} \right)^y \quad (3)$$

$$SC_{COST} = \sum_{i=1}^{n_{cap}} Q_{cap,i} \times IC_{cap} + MC_{cap} \times \sum_{y=1}^{N_{yrs}} \left( \frac{1 + \text{inf}R}{1 + \text{int}R} \right)^y \quad (4)$$

$Q_{cap,i}$  denotes the  $i$ th shunt capacitors size in MVAR,  $IC_{cap}$  represents the SC cost of investment in \$/MVAR,  $n_{cap}$  specifies the total amount of SC placed in the RDN, the annual maintenance cost is denoted with  $MC_{cap}$ ,  $N_{yrs}$  represents the total quantity of planning years (npy),  $\text{inf}R$  represents the inflation rate, and  $\text{int}R$  is the interest rate.

### B. Evaluation of Switch Cost

The switching cost is comprised of the capital investment (that includes the installation charges) as well as the annual maintenance and operation expenses. Below is a mathematical assessment of it [31].

$$SW_{Cost} = \sum_{s=1}^{N_s} S_{inv,s}^{Cost} + \sum_{s=1}^{N_s} S_{O\&M,S}^{Cost} \times \sum_{y=1}^{N_{yrs}} \left( \frac{1 + \text{inf}R}{1 + \text{int}R} \right)^y \quad (5)$$

Where  $S_{inv,s}^{Cost}$  is the investment cost of switch,  $S_{O\&M,S}^{Cost}$  represents the switch maintenance and operation cost, and  $N_s$  is the quantity of switches that must be added to the network. The best sectionalizing switch

### C. Cost-benefit analysis based on the lower energy costs

Utilities procure energy from the transmission grid to meet end customers' power demands; however, feeder line losses cause part of this power to be lost. Reference [32] provides the purchasing price ( $PP_{Grid}^{Before}$ ) of power from the substation prior to reconfiguration and SC integration.

$$PP_{Grid}^{Before} = C_{Grid} \times (P_{Grid}^{Before} + P_{loss}^{Before}) \times T \quad (6)$$

Where  $C_{Grid}$  is the cost of grid-supplied electricity in \$/MWh,  $P_{Grid}^{Before}$  (in MW) denotes the substation's cumulative active power supplied before SC allotment, and  $P_{loss}^{Before}$  typifies the overall active power loss before SC allotment.

The utilities can reduce system energy losses and partially satisfy system power demand through effective SC deployment. Consequently, following reconfiguration and SC integration, the price of purchasing power from the substation, accounting for power loss,  $PP_{Grid}^{After}$  is given by:

$$PP_{Grid}^{After} = C_{Grid} \times (P_{Grid}^{After} + P_{loss}^{After}) \times T \quad (7)$$

Where  $P_{Grid}^{After}$  represents the total active power (in MW) that the substation injects at bus 1 following the reconfiguration and integration of SC, and  $P_{loss}^{After}$  is the total active power loss (in MW).

Therefore, after reconfiguration and the allotment of SCs, the cost-benefit ( $CB_p$ ) resulting from the decreased price of electricity purchased via the sub-station, considering energy loss, as shown by ref. [36]

$$CB_p = PP_{Grid}^{Before} - PP_{Grid}^{After} \quad (8)$$

Substituting (6) and (7) in (8), then;

$$CB_p = C_{Grid} \times \left[ (P_{Grid}^{Before} - P_{Grid}^{After}) + (P_{loss}^{Before} - P_{loss}^{After}) \right] \times T \quad (9)$$

The evaluation of the Present Worth Factor (PWF) for (6), (7), and (9):

$$PWF(PP_{Grid}^{Before}) = PP_{Grid}^{Before} \times \sum_{y=1}^{N_{yrs}} \left( \frac{1 + \text{inf}R}{1 + \text{int}R} \right)^y \quad (10)$$

$$PWF(PP_{Grid}^{After}) = PP_{Grid}^{After} \times \sum_{y=1}^{N_{yrs}} \left( \frac{1 + \text{inf}R}{1 + \text{int}R} \right)^y \quad (11)$$

$$PWF(CB_p) = CB_p \times \sum_{y=1}^{N_{yrs}} \left( \frac{1 + \text{inf}R}{1 + \text{int}R} \right)^y \quad (12)$$

### D. Evaluation of the total cost-benefits ( $CB_T$ )

Ultimately, the variety of SC costs and switching costs discussed in the preceding subsection are carefully considered to create a single, distinct objective function that is stated as follows:

$$CB_T = PWF(CB_p) - (PWF(SW_{Cost}) + SC_{COST}) \quad (13)$$

Where  $CB_T$  is the cumulative cost-benefit throughout the quantity of planning years ( $N_{yrs}$ ) attained by network reconfiguration and optimal SC allotment.

Having obtained the objective function's complete mathematical representation. Finally, it can be expressed as;

$$OF_{max} = CB_T = PWF(CB_p) - (PWF(SW_{Cost}) + SC_{COST}) \quad (14)$$

## 2. Constraints

The following constraints are applicable to the objective function:

### A. Power flow equations

During the optimization phase, the direct load flow (DLF) approach is utilized when solving the power flow equation. The following are the equations:

$$P_{gi} = P_{Di} + \sum_{j=1}^{n_b} |V_i||V_j| [G_{ij}\cos\theta_{ij} + B_{ij}\sin\theta_{ij}] \quad (15)$$

$$Q_{gi} = Q_{Di} + \sum_{j=1}^{n_b} |V_i||V_j| [G_{ij}\sin\theta_{ij} - B_{ij}\cos\theta_{ij}] \quad (16)$$

where buses "i" and "j" have voltages of  $V_i$  and  $V_j$ , respectively; The generated and demanded active power at bus "i" is represented by  $P_{gi}$  and  $Q_{Di}$ ; reactive power produced and requested at bus "i" is represented by  $Q_{gi}$  and  $Q_{Di}$ ; and the difference in voltage phases between buses "i" and "j" is represented by  $\theta_{ij}$ .

### B. Reactive Power Compensation Limit

Shunt capacitors' maximum permissible compensation limit should not be higher than the network's overall reactive load. It can be expressed utilizing the equation below:

$$\sum_{i=1}^{n_{cap}} Q_{cap,i} \leq TotalQ \quad (17)$$

### C. Bus voltage constraint

The voltage needs to be within the RDN standard limits.

$$V_{min} \leq V_i \leq V_{max} \quad (18)$$

$V_{min}$  denotes the minimum voltage ( $V_{min} = 0.95$ ),  $V_{max}$  represents the maximum voltage ( $V_{max} = 1.05$ ), and the bus voltage is denoted by  $V_i$ .

### D. Thermal Constraints

Eq. (19) states that the current flow ( $I_i$ ) via the RDN's distribution

lines cannot exceed the allowable loading capacity ( $I_{max,i}$ ).

$$|I_i| \leq |I_{max,i}|; i = 1, 2, \dots, N_B - 1 \quad (19)$$

#### E. Radial configuration constraint

To ensure that energy only flows in one direction to every bus connected to the network, the RDN's radial structure must be preserved.

#### 3. Average Voltage Stability Index (AVSI)

In addition to being vulnerable to voltage instability, RDNs can breakdown under load and stress. Utilizing the VSI, busses that need to be compensated for their potential to collapse are identified [37]. It is provided as follows:

$$VSI = |V_s|^4 - 4[P_r R_{sr} + Q_r X_{sr}] |V_r|^2 - 4[P_r R_{sr} + Q_r X_{sr}] \quad (20)$$

The subscripts "s" and "r" stand for "from" and "to" bus. Real power is denoted by  $P$  and reactive power by  $Q$ , and the bus voltage is represented by  $V$ .  $R$  and  $X$  typifies the distribution lines' resistance and reactance, respectively. When all distribution line VSIs are added together and divided by the cumulative quantity of distribution lines, the resulting total VSI is known as the average VSI (AVSI), and it can be shown as follows:

$$AVSI = \left( \frac{\sum_{i=1}^{N_b-1} VSI_i}{N_b - 1} \right) \quad (21)$$

#### 4. Voltage Profile Index

An index was employed to indicate the extent to which the voltage matches the nominal value in order to contrast the voltage profiles under various conditions [38]. The mathematical expression for VPI is Eq. (22).

$$VPI = \log_{10} \left( C \times \left| \frac{1}{V_\beta - 1} \right| \right) \quad (22)$$

$V_\beta$  and  $C$  can be obtained as follows:

$$V_\beta = \frac{1}{N} \sum_{j=1}^N V_j \quad (23)$$

$$C = 1 - V_\chi \quad (24)$$

$$V_\chi = \sqrt{\frac{1}{N} \sum_{j=1}^N (V_j - V_\beta)^2} \quad (25)$$

Where,

$N$  denotes the total quantity of buses,  $V_j$  represents voltage magnitude at bus  $j$ ,  $V_\beta$  denotes the average bus voltage, and  $V_\chi$  represents the standard deviation of the bus voltages, and  $C$  is the difference between unity and the standard deviation of the bus voltages.

Considering two scenarios (A and B), if  $VPI_A > VPI_B$ , then a better voltage profile is offered by scenario A.

### 3. Proposed algorithm

#### 3.1. Overview of the DO algorithm

The DO is an advanced metaheuristic algorithm inspired by the natural dispersal process of dandelion seeds. It was proposed and mathematically modelled by Zhao et al., (2022) [39]. With its roots in

swarm intelligence, this innovative optimization technique mimics the flight of dandelion seeds in search of fertile ground. By harnessing principles from nature, the Dandelion Optimizer efficiently explores complex solution spaces, finding a balance between exploitation and exploration. Its versatility and effectiveness make it a promising tool for tackling diverse optimization challenges across various domains. The flight of the dandelion seeds are modelled to go through three stages; rising, descending, and landing stages.

#### 3.1.1. Initialization

During the dandelion population's initialization phase, DO uses Eq. (26) to arbitrarily create each candidate solution. where  $Dim$  and  $pop$  stand for the values representing variable dimension and population size, respectively.  $LB = (lb_1, lb_2, \dots, lb_{Dim})$  and  $UB = (ub_1, ub_2, \dots, ub_{Dim})$  denotes the seed status's upper and lower bounds, respectively.

$$X_{i,j} = rand \times (ub_j - lb_j) + lb_j, i = 1, 2, \dots, pop, j = 1, 2, \dots, Dim \quad (26)$$

After initialization, the seed with the lowest fitness is picked as the dandelion seed propagation's best location, and is denoted as  $X_{elite}$ . The  $i$ th seed's fitness score in the population is denoted by  $f(X_i)$ . The expression goes like this:

$$f_{best} = \min(f(X_i))$$

$$X_{elite} = X(\text{find}(f_{best} = f(X_i))) \quad (27)$$

where an index that has two identical values is indicated by  $\text{find}()$ .

#### 3.1.2. Rising stage

The growing altitude of dandelion seeds is determined by a combination of wind speed and meteorological conditions throughout the ascending phase, which is why the weather is categorized as sunny or rainy.

Case 1. *In bright days, wind speed follows a log-normal distribution; dandelion seeds have higher chances of travelling long distances under this distribution. Thus, on bright days, the DO promotes exploration. The vortex over the dandelion seeds is continually shifting due to wind speed, which causes the seeds to spiral upward. The model depicting the upward spiraling dandelion seeds on a sunny day is described below:*

$$X_i^{t+1} = X_i^t + \alpha^* s_x^* s_y^* \ln Y^* (X_s^t - X_i^t) \quad (28)$$

$$X_s^t = rand(1, Dim)^* (UB - LB) + LB, \quad (29)$$

$$\alpha = rand()^* \left( \frac{1}{T^2} t^2 - \frac{2}{T} t + 1 \right), \quad (30)$$

$$r = \frac{1}{e^\theta},$$

$$s_x = r^* \cos\theta, \quad (31)$$

$$s_y = r^* \sin\theta,$$

Where the seed's position at iteration  $t$  is depicted by  $X_i^t$ . The random location of dandelion seeds at iteration  $t$  is depicted by the symbol  $X_s^t$ . The highest possible number of iterations is  $T$ . To indicate a log-normal distribution,  $\ln Y$  is used. Obeying  $\mu = 0, \sigma^2 = 1, \alpha$  is an adaptive parameter,  $\hat{T}$  is a random value in  $[-\pi, \pi]$ ,  $s_x$  and  $s_y$  are the coefficients of the dandelion seed lift component.

Case 2 *On wet days, the breeze does not cause dandelion seeds to rise. The dandelion seeds currently highlight neighborhood exploitation on a local level. Below is the appropriate model and formula:*

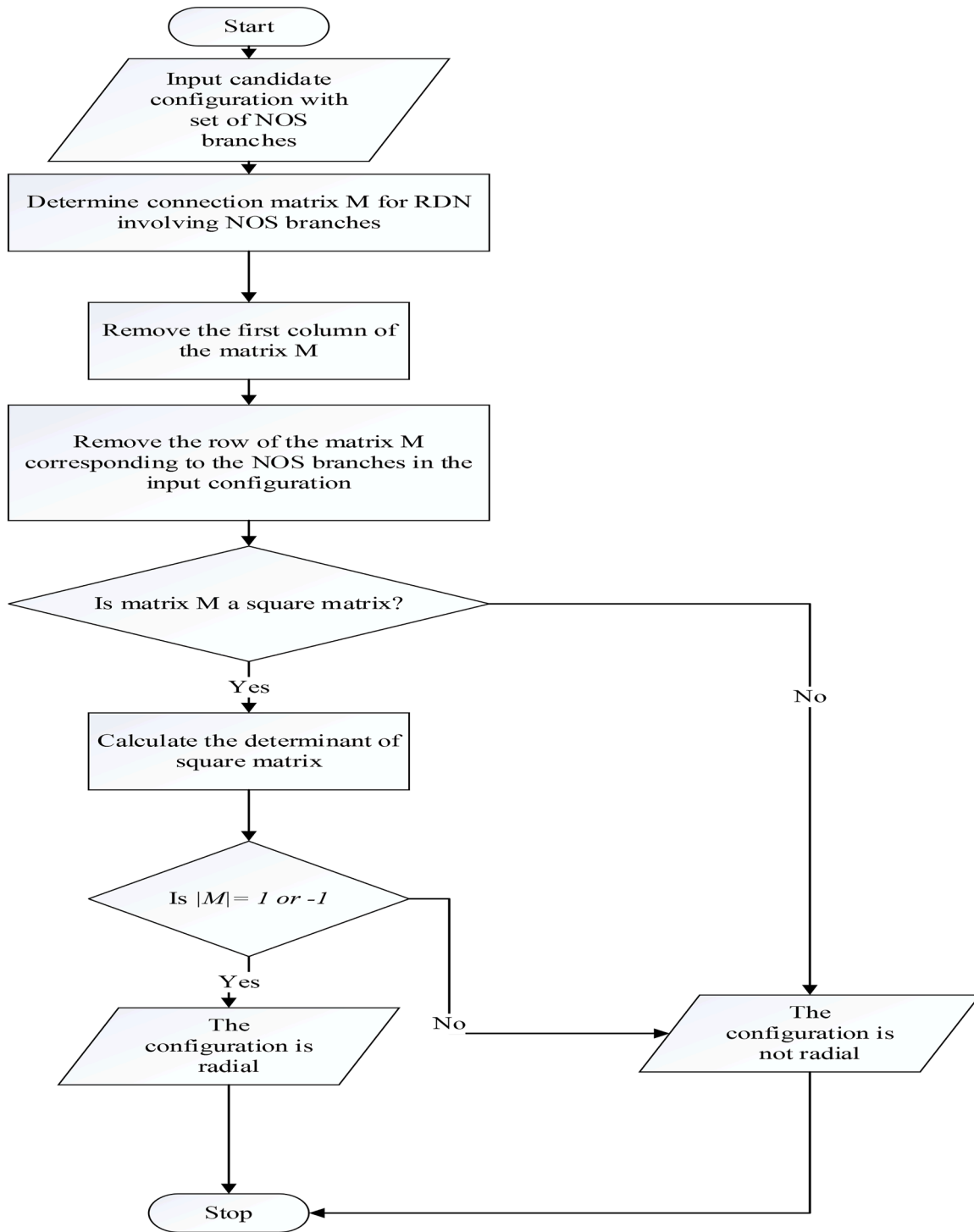


Fig. 1. Radiality check for candidate configuration.

$$e = T^2 - 2T + 1, \tag{32}$$

$$\beta = 1 - rand() \cdot \frac{1}{e} (t^2 - 2t - 1), \tag{33}$$

$$X_i^{t+1} = X_i^t \cdot \beta, \tag{34}$$

The local adaptive parameter is typified using  $\beta$ , the highest iteration number us denoted using  $T$ .

In conclusion, the following is the mathematical depiction of the rising phase for dandelion seeds:

$$X_i^{t+1} = \begin{cases} X_i^t + \alpha \cdot s_x \cdot s_y \cdot \ln Y^* (X_s^t - X_i^t) \cdot randn < 1.5 \\ X_i^t \cdot \beta \text{ else} \end{cases} \tag{35}$$

*randn* denotes an arbitrary number after standard normal distribution.

### 3.1.3. Descending stage

In the decline stage, DO prioritizes global exploration. In addition to reflecting the stability of the fall, utilizing the mean location after the

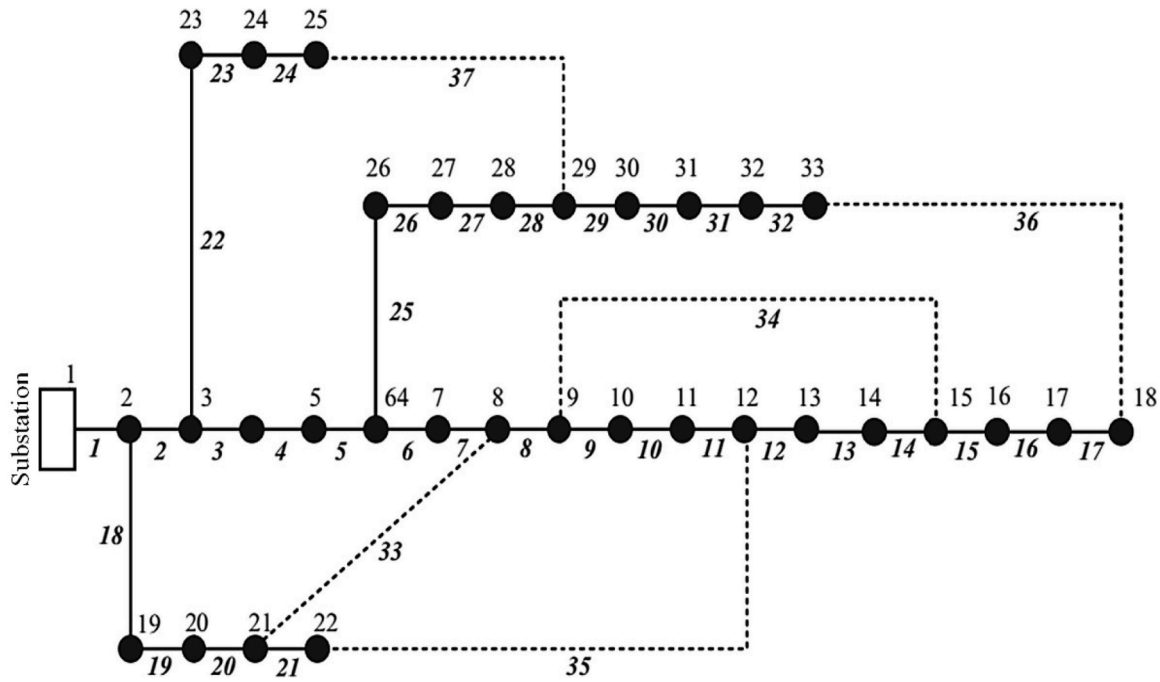


Fig. 2. Single-line diagram of the IEEE 33-bus RDN.

Table 1  
Grid features and cost specifications.

Parameters	Symbols	Value
Investment cost of SC	$SC_{inv\_cost}$	4000 (\$/MVar)
SC annual maintenance cost	$SC_{MC}$	10% of $SC_{inv\_cost}$
Investment cost of Tie Switch	$S_{inv\_s}^{Cost}$	4700 (\$)
Tie switch operation and maintenance cost.	$S_{O\&M,S}^{Cost}$	2% of $S_{inv\_s}^{Cost}$
Power purchase cost from Disco	$C_{grid}$	49 (\$/MWh)
Planning years	$N_{yrs}$	20 years
Time (No of hours in a year)	T	8760 hours
Interest rate	$IntR$	12.5 %
Inflation rate	$InfR$	9.5 %

Table 2  
Simulation Results for IEEE 33-Bus RDN.

	Base case	Rec only	SCA only	Rec and SCA
SC size in kVar (location)			301(14) 492 (7) 907 (30)	430(24) 191(22) 167(7)
Open branches	33 34 35 36 37	27 15 37 36 7	33 34 35 36 37	27 7 37 36 15
Ploss (kW)	210.99	93.09	139.63	78.28
%Ploss		55.88	33.82	62.90
Qloss (kVar)	143.13	77.30	95.31	65.18
SC cost (\$/npy)			16,721.20	7750.76
Switch cost (\$/npy)		24,285.84		24,285.84
VPI (p.u)	1.2477	1.8758	1.4196	1.9374
AVSI (p.u)	0.8124	0.9517	0.8678	0.9580
Cost-benefit (\$/npy)		707,985.06	430,128.64	765,535.27
Vmin (p.u.)	0.9038(18)	0.9728(33)	0.9339 (18)	0.9728 (33)

growing phase aids the population of dandelion seeds in moving toward the most productive area. The following is the mathematical model that represents the declining phase:

$$X_{mean\_t} = \frac{1}{pop} \sum_{i=1}^{pop} X_i, \quad (36)$$

$$X_i^{t+1} = X_i^t - \alpha^* \beta_t^* (X_{mean\_t} - \alpha^* \beta_t^* X_i^t), \quad (37)$$

Where  $X_{mean\_t}$  typifies the average location of the dandelion numbers in  $ith$  iteration, Brownian motion is  $\beta_t$ .

### 3.1.4. Landing stage

Local community development is the DO's primary objective throughout the landing phase. The dandelions seeds determine where to land at random based on the rising and falling phases. To get closer to the global optimum, local exploitation is conducted using the data pertaining to the current elite seed. The corresponding mathematical model for the landing stage is:

$$X_i^{t+1} = X_{elite} + levy(\lambda)^* \alpha^* (X_{elite} - X_i^{t+1} * \delta), \quad (38)$$

$$\delta = \frac{2t}{T} \quad (39)$$

T is the largest number of iterations that can be performed, and  $X_{elite}$  represents the most favorable seed position at iteration t.

### 3.2. Radial configuration check

A configuration check is performed to ensure that the radial configuration requirements are met at various stages of the proposed technique's optimization process. This is done before the loading flow is executed and the fitness value of each generated solution is ascertained. In every configuration, the incidence matrix M is located. The first column, where in the RDN corresponds to the slack bus is to be eliminated to create a square matrix M. There are two values for the square matrix M determinant, which indicate radial or non-radial arrangements [40]. The radial feasibility flowchart for the setup is displayed in Fig. 1.

### 3.3. Application of DO for RDNR and SCA

The steps involved are as follows:

**Step 1:** Input the parameters for the tie switches and DO, as well as the line and load data for the RDN.

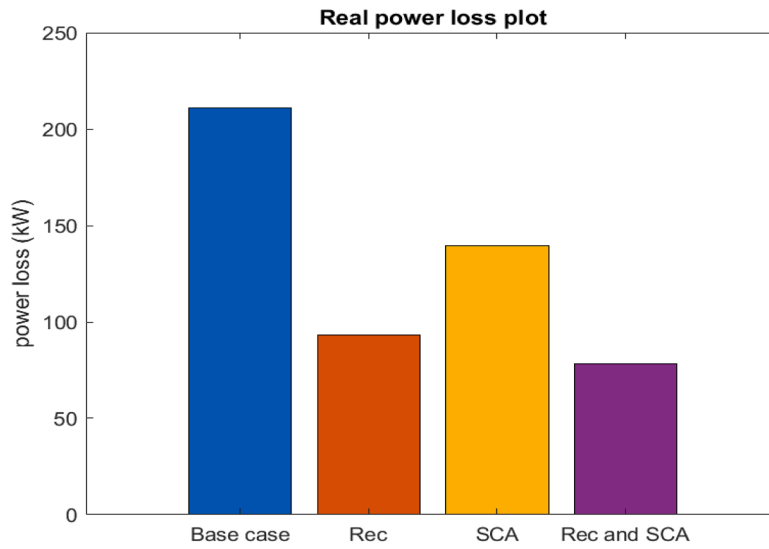


Fig. 3. Active power loss plot for all considered cases for IEEE 33-bus RDN.

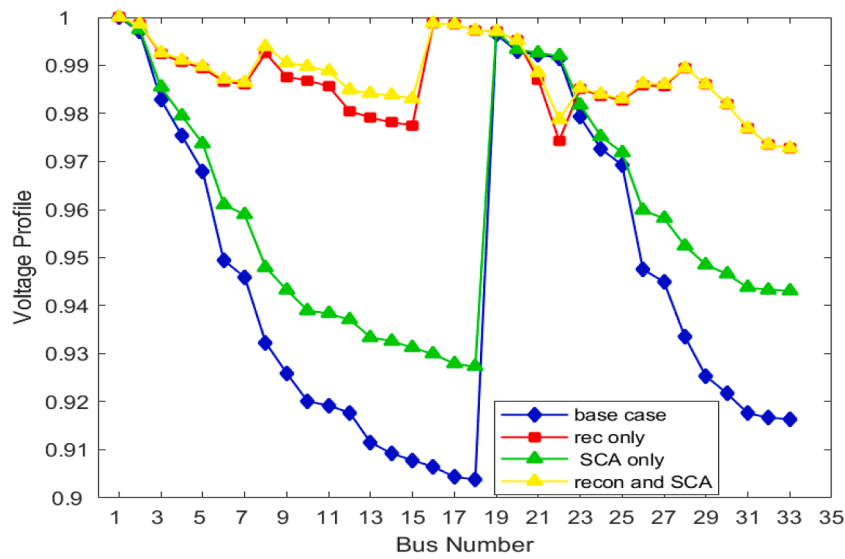


Fig. 4. Voltage profile plot for all considered cases for IEEE 33-bus RDN.

**Step 2:** Determine the RDN’s fundamental loops (FLs).

**Step 3:** Depending on branches’ size that make up each tie-switch’s corresponding FL, initialize the dandelion seeds (X) of its DO. A dandelion seed is a possible solution consisting of NOBs, SC locations and SC sizes. A rise of  $n$  dandelions is expressed as:

$$D = \begin{bmatrix} d_1 \\ d_2 \\ \vdots \\ d_n \end{bmatrix} = \begin{bmatrix} NOS_1^1, \dots, NOS_{NTL}^1 & loc.SC_1^1, \dots, loc.SC_m^1 & size.SC_1^1, \dots, size.SC_m^1 \\ NOS_1^2, \dots, NOS_{NTL}^2 & loc.SC_1^2, \dots, loc.SC_m^2 & size.SC_1^2, \dots, size.SC_m^2 \\ \vdots & \vdots & \vdots \\ NOS_1^n, \dots, NOS_{NTL}^n & loc.SC_1^n, \dots, loc.SC_m^n & size.SC_1^n, \dots, size.SC_m^n \end{bmatrix} \quad (40)$$

Every seed in the flight is represented by:

$$d_i = [NOS_1^i, \dots, NOS_{NTL}^i \quad loc.SC_1^i, \dots, loc.SC_m^i \quad size.SC_1^i, \dots, size.SC_m^i] \quad (41)$$

Eq. (41) makes clear that each seed’s solution vector is composed of three components. The number of busses chosen for SC penetration is represented by the second component, the number of commonly open switches or lines (open branches: NOSs) of the RDN is represented by the first part, and the sizes of the SC units are represented by the third part.

From the expressions,  $NOS_1, NOS_2, \dots, NOS_{NTL}$  denotes the normally open switches (open branches) in the fundamental loops,  $loc.SC_1^i, \dots, loc.SC_m^i$  stands for the optimal busses selected for reactive compensations;  $size.SC_1^i, \dots, size.SC_m^i$  represents the capacities of the SCs in kVAR to be allotted at the chosen busses, respectively.

Every dandelion in the DO can be seen of as a randomly generated initialization solution. As a result, every seed in the population is initialized at random in this way:

$$NOS_i = round \left[ NOS_{lower,r1}^i + rand \times (NOS_{upper,r1}^i - NOS_{lower,r1}^i) \right] \quad (42)$$

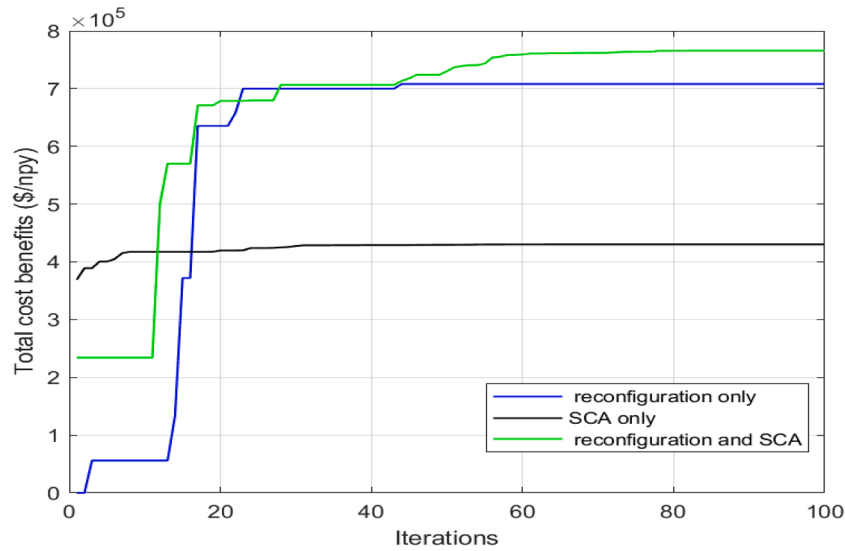


Fig. 5. Convergence characteristics for all considered cases for IEEE 33-bus RDN.

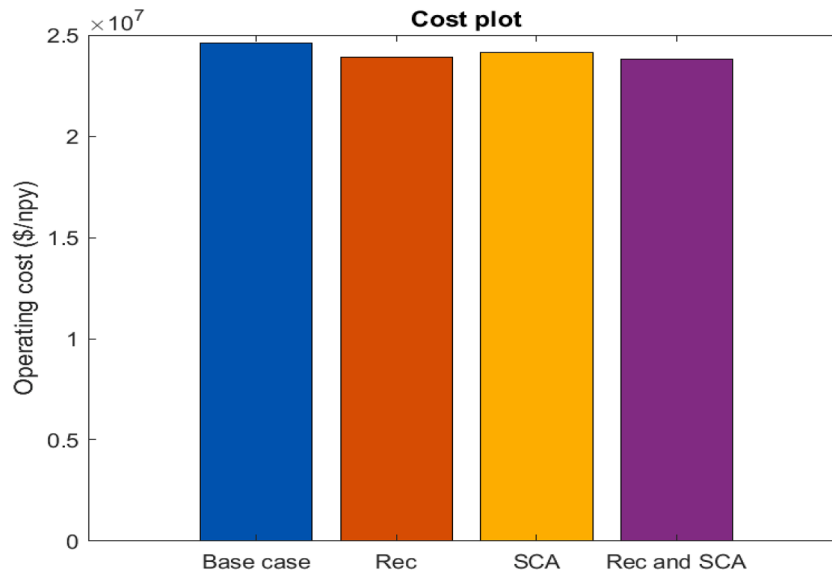


Fig. 6. Operating costs for all considered cases for IEEE 33-bus RDN.

$$loc.SC_i = round \left[ loc_{lower,r2}^i + rand \times \left( loc_{upper,r2}^i - loc_{lower,r2}^i \right) \right] \quad (43)$$

$$size.SC_i = round \left[ size_{lower,r3}^i + rand \times \left( size_{upper,r3}^i - size_{lower,r3}^i \right) \right] \quad (44)$$

With the exception of the slack bus, which serves as the first bus, SCs can be installed at any bus of the RDN. As a result, according to the inequality constraints of Eq. (17), the SC units' lowest and highest limits are from bus 2 to the RDN's last bus, and the sizes of each SC range from 100kVAr to the maximum total reactive load of the network.

- Step 4:** Utilizing the direct load flow technique, obtain the total power loss, the total operating costs and bus voltages.
- Step 5:** Obtain the position and size of the SCs by calculating the fitness value (f) of each dandelion seed. Create a size that meets every optimization constraint.
- Step 6:** Based on fitness values, choose the best dandelion seed.
- Step 7:** Initialize the counter.

**Step 8:** Execute the power flow analysis, obtain the power loss for every seed produced, and assess its corresponding fitness values utilizing the modelled objective function.

**Step 9:** While (t < T), do /\*Rise stage\*/

**Step 10:** Calculate the exploitation between the previous position and the elite seed.

**Step 11:** Make use of Eq. (30) to generate adaptive parameters.

**Step 12:** Utilizing Eq. (34), update dandelion seeds.

**Step 13:** End if /\*Decline stage\*/. Else, go to step 12

**Step 14:** Utilizing Eq. (37) for /\*Land stage\*/, update dandelion seeds

**Step 15:** Utilizing Eq. (27), update  $X_{elite}$

**Step 16:** Print the results.

### 3.4. Overview of methodology, operational details, and system configurations

Buses in RDNs are connected through sectionalizing switches and tie switches, which are normally closed and normally open, respectively,

**Table 3**  
Comparison with Other Techniques for IEEE 33-Bus RDN.

Technique	Open branches	SC (kVAr)/ bus	Power loss (kW)	% Power loss reduction	Min. Bus Voltage (p.u)
Base case	33 34 35 36 37		210.99		0.9131
Scenario 2: Reconfiguration only					
MBA [28]	7 14 9 32 37		139.53	31.14	N.A.
ICSA [44]	7 14 9 32 37		139.55	31.14	0.9378
HSA [28]	7 14 9 32 37		139.55	31.14	0.9378
FWA [28]	7 14 9 32 28		139.98	30.93	0.9413
ACSA [45]	7 14 9 32 28		139.55	31.14	0.9413
HM [46]	7 9 14 32 37		139.55	30.93	0.9378
UVDA [28]	7 9 14 32 37		139.55	31.14	0.9378
INNA [47]	7 9 14 32 37		139.55	31.14	0.9378
ACA [28]	7 9 14 32 37		139.68	31.07	0.9375
SFS [48]	7 14 9 32 37		139.55	31.14	0.9378
GWO [28]	7 14 9 32 37		139.55	31.14	0.9378
DO	27 15 37 36 7		93.09	55.88	0.9728
Scenario 3: SCA only					
AWOA [25]	33 34 35 36 37	150 (24) 50 (25) 150 (30)	115.88	31.82	N.A.
LS [25]	33 34 35 36 37	450 (12) 350 (25) 900 (30)	139.23	31.30	N.A.
MLIP [9]	33 34 35 36 37	750 (6) 150 (28) 850 (29)	139.57	31.13	0.9302
ACA [28]	33 34 35 36 37	600 (9) 450(28) 600 (29)	136.14	32.82	N.A.
DO	33 34 35 36 37	301 (14) 492 (7) 907 (30)	139.63	33.82	0.9339
Scenario 4: Simultaneous reconfiguration and SCA					
GWO [28]	7 9 14 32 37	533 (24) 957 (30) 445 (8)	92.59	54.31	0.9595
ACA [28]	7 9 14 32 37	600 (20) 450 (28) 600 (29)	95.79	52.73	0.9656
BFO [28]	7 11 34 37 36	600 (5) 300 (16) 300 (25)	101.08	50.12	0.9712
AWOA [25]	33 34 35 36 25	400 (2) 250 (25) 150 (30)	97.415	42.68	N.A.
MBBO [49]	7 11 34 36 28	750 (27) 450 (30) 600 (24)	83.47	58.82	N.A.
CS [49]	8 5 37 30 12	300 (8) 750 (30) 600 (23)	95.66	52.80	N.A.
MIC [25]	9 25 14 33 37	750 (27) 150 (2) 750 (24)	97.64	51.83	N.A.

**Table 3 (continued)**

Technique	Open branches	SC (kVAr)/ bus	Power loss (kW)	% Power loss reduction	Min. Bus Voltage (p.u)
APSO [9]	7 9 14 32 34	516 (24) 624 (21) 961 (30)	92.64	54.30	0.9585
DO	27 7 37 36 15	430 (24) 191 (22) 167 (7)	78.28	62.90	0.9728

under standard system operations. These switches are used to maintain the radial nature of the distribution systems, ensuring a unidirectional power flow to each bus. Under operation, current demand from buses, particularly the ones with high power-consuming loads, leads to high power losses in the systems due to the distribution lines' impedances. Hence, the more impeditive the distribution paths to these loads are from the slack bus, the higher the system losses. High system losses correspondingly lead to poor cost efficacy of the RDNs, which is then prioritized as the objective of this research. The reconfiguration procedure alters the topology of the network by developing new tie switches (opening some of the existing sectionalizing switches and closing some of the existing tie switches) that provide the path with the least impedance to buses with high power-consuming load, thereby reducing power losses, maximizing cost benefits, and improving voltage profiles. The optimization model in this work finds this optimal configuration and determines the location and sizes of SCs to be integrated into the network for reactive compensation and additional voltage profile enhancement. The algorithm in Fig. 1 ensures the system stays radial through every configuration in the optimization process. The SCs selected for integration in this study are single capacitors. While single capacitors are known to possess fixed and limited reactive power capacities, it is selected in this study due to their ease of installation, flexibility, and, most importantly, their relatively low investment costs, which is further aimed at maximizing the objective function specified in this study. Further diagrammatical explanations about the switch details and the base case system configurations of the test networks considered in this study can be seen in Figs. 2 and 7.

**4. Results and discussion**

The IEEE 33-bus and IEEE 69-bus RDN test beds are utilized to implement and validate the novel DO technique described in this research study. The bounds of the capacitor sizes chosen for allotment in the test beds ranges between 150 and 1500 kVAR and the minimum and maximum bus voltages for all cases considered is  $V_{max} = 1.05$  p.u and  $V_{min} = 0.9$  p.u. The direct load flow technique proposed by Teng [41] was used. In the mesh distribution network, the reconfiguration process starts with every switch closed. To break loops, one at a time, each switch is opened. The maximizing of total cost benefits is the condition for opening a switch and the switch that yields the optimal cost-benefit should be opened. Additionally, only SC sizes that maximizes the cost benefits should be integrated. Table 1 presents the parameters utilized in the mathematical derivations of the objective function.

Using a 3.0 GHz, 64-bit PC with an i5 processor and 8 GB RAM, MATLAB® software is utilized to obtain the load flow solution and the DO-based approach. The total number of search agents is set at 30, and the total iteration number is fixated at 100.

The following scenarios are examined for each test beds, and comparisons are made with the findings found in recent researches.

**Scenario 1:** Base case (before NR an SC allotment)

**Scenario 2:** Only Reconfiguration.

**Scenario 3:** Only SC allotment.

**Scenario 4:** Reconfiguration coupled with SC allotment.

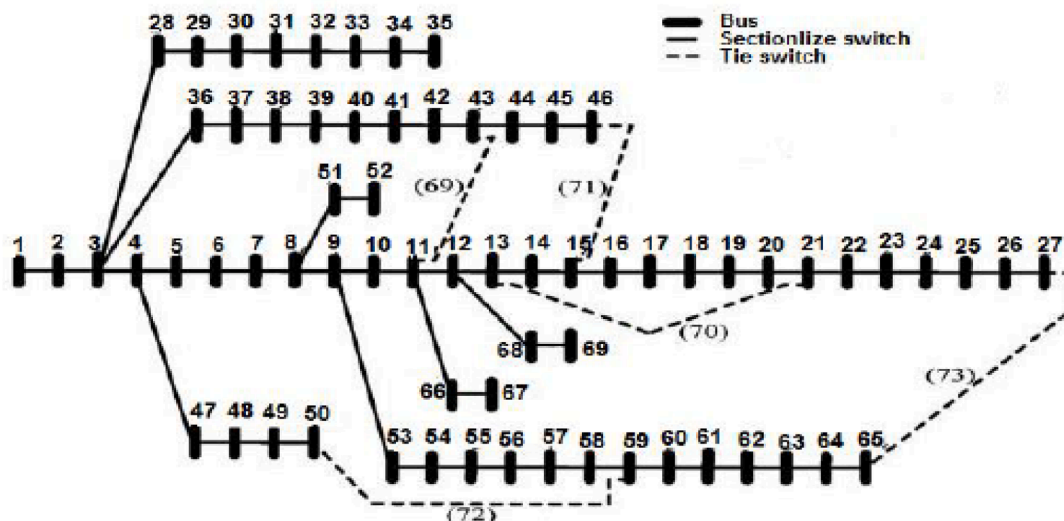


Fig. 7. Single line-diagram of the IEEE 69-bus RDN.

**Table 4**  
Simulation results for IEEE 69-Bus RDN.

	Base case	Rec only	SCA only	Rec and SCA
SC size in kVar (location)			878 (61)	150(21)
			204 (64)	150(6)
			179 (21)	150(59)
Open branches	69 70 71 72 73	73 58 60 71 69	69 70 71 72 73	45 11 10 23 60
Ploss (kW)	224.99	58.82	144.36	43.80
%Ploss		73.86	35.83	80.51
Qloss (kVar)	102.16	37.95	69.65	35.22
SC cost (\$/npy)			12 403.12	4 426.20
Switch cost (\$/npy)		30 357.30		30 357.30
VPI (p.u)	1.5866	2.1674	1.6530	2.4680
AVSI (p.u)	0.9062	0.9627	0.9222	0.9874
Cost-benefit (\$/npy)		1 010 300.87	473 641.32	1 134 722.60
Vmin (p.u.)	0.9092(65)	0.9712 (27)	0.9283 (65)	0.9899 (59)
				0.9900

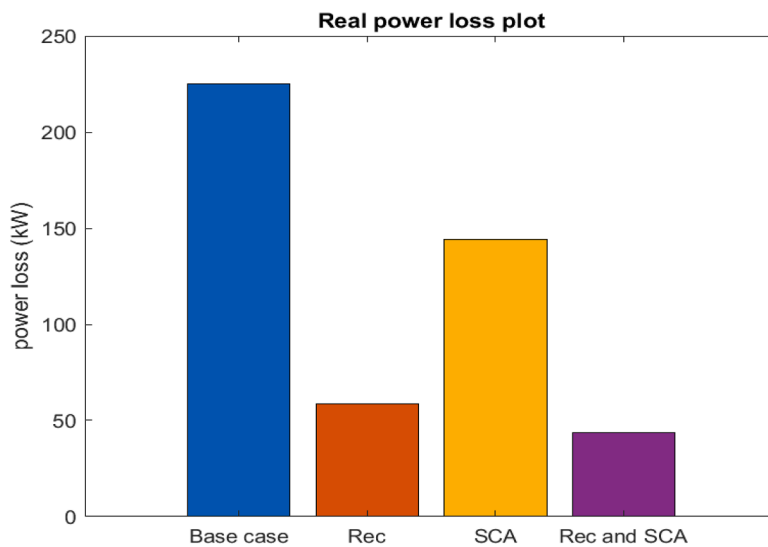


Fig. 8. Active power loss plot for all considered cases for IEEE 69-bus RDN.

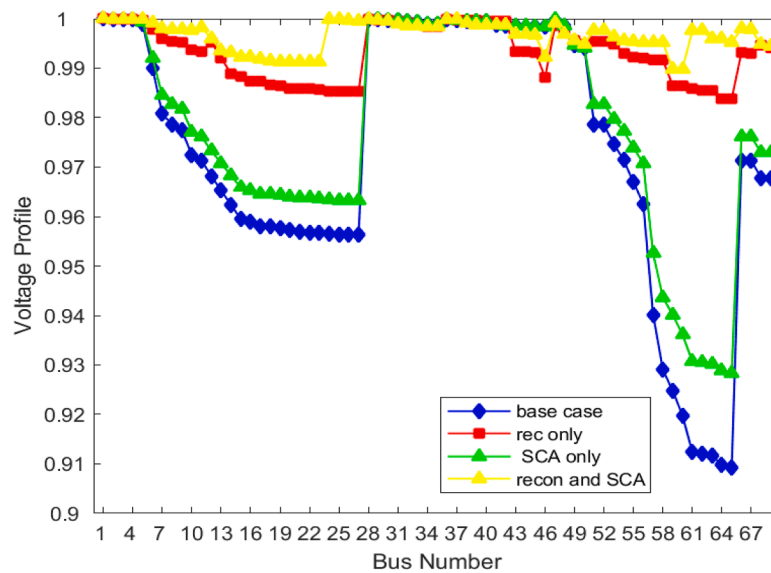


Fig. 9. Voltage profile plot for all considered cases for IEEE 69-bus RDN.

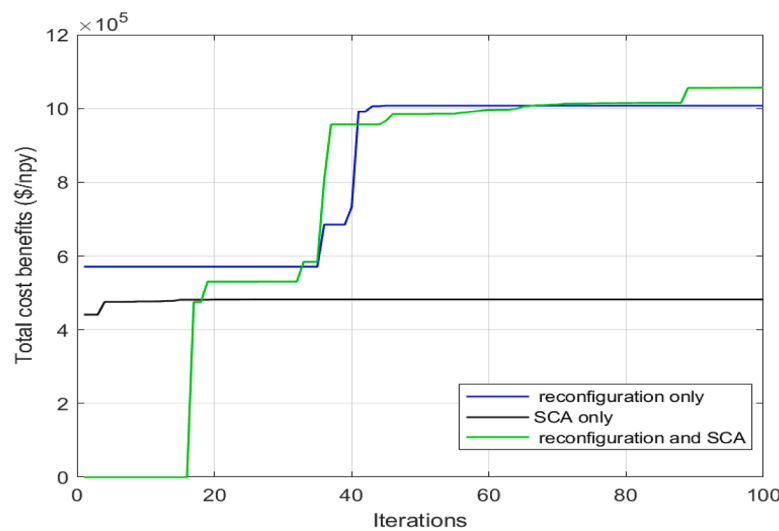


Fig. 10. Convergence characteristics for all considered cases for IEEE 69-bus RDN.

#### 4.1. IEEE 33-Bus RDN

The IEEE 33-Bus RDN is operated at 12.66kV with load requiring total real power and reactive power of 3.7150MW and 2.300 MVar, respectively. The RDNs' line and load data can be obtained from [42]. 37 branches made up of 32 normally closed branches (NCB) and 5 normally opened branches (NOB) can be found in the 33-bus RDN, with its initial tie switches located at branches [33–37]. The base case results obtained after load flow depicts the cumulative active power, reactive power loss, VPI and AVSI to be 210.99 kW, 143.13kVAr, 1.2477 p.u and 0.8124 p.u, respectively. Its line diagram is shown in Fig. 2.

Table 2 showcase the results obtained for all cases returned by the DO optimizer for its cost-based objective function. Considering scenario 2(after NR only), the newly acquired open branches are [27,15,37,36,7], which have 77.30 kVAr for reactive power and 93.09 kW for active power losses, respectively, which is quite low. The active power loss corresponds to 55.88 % reduction in comparison with the value of the base case (210.99 kW) before changes in the system. The lowest voltage magnitude in p.u was obtained to be 0.9728 at bus 33, with VPI and AVSI values of 1.8758 and 0.9517, respectively. The switch cost and the

total cost benefit 24 285.84(\$/npy) and 707 985.06 (\$/npy) were incurred by the reconfiguration procedure.

For case 3 (SCA only), the algorithm returned shunt capacitors sizes (kVAr) of 301,492 and 907 situated at buses 14,7 and 30 respectively, with a reduced active and reactive power losses of 139.63kW and 95.31kVAr which corresponds to a 33.82 % and 33.41 % diminution in the active and reactive power losses, respectively in relation to the base case. The obtained value for the minimum voltage magnitude, VPI and AVSI in p.u were 0.9339 at bus 18, 1.4196 and 0.8678, respectively. Finally, the total cost benefit incurred and Shunt Capacitor cost by the Shunt capacitor allocation were obtained to be 430 128.64 (\$/npy) and 16 721.20 (\$/npy)

Proceeding to case 4 (simultaneous NR and SCA), the new open branches obtained were found to be [27,7,37,36,15] and the shunt capacitor sizes in kVAr were obtained to be 430,191 and 167 located at buses 24, 22 and 7, respectively. The active and reactive power losses were found to be 78.28 kW and 65.18 kVAr, respectively which correlates to a 62.90 % reduction in active power loss and 54.46 % reduction in reactive power loss on comparison with the base case. The minimum voltage magnitude in p.u was 0.9728 at bus 33, and VPI and AVSI were

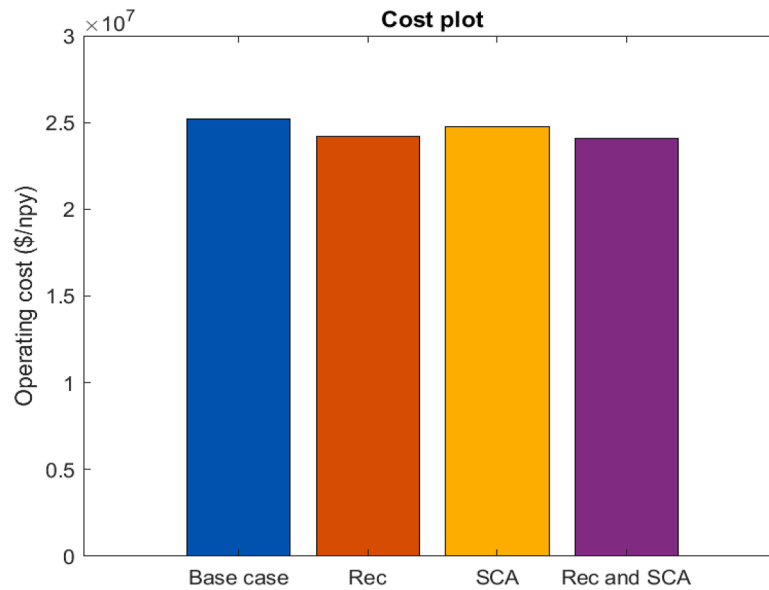


Fig. 11. Operating costs for all considered cases for IEEE 69-bus RDN.

1.9374 and 0.9580, respectively. Conclusively, the total cost-benefit, switch cost and shunt capacitor cost incurred by the synchronous reconfiguration of the RDN and shunt capacitors integrations were computed at 765 535.27 (\$/npy), 24 285.84(\$/npy) and 7 750.76 (\$/npy), respectively. Figs. 3, 4, 5, and 6 explain diagrammatically the notable improvements obtained on the RDN for all cases considered in terms of active power loss reduction, voltage profile enhancement, convergence characteristics, and the total reductions in operating costs, respectively when compared to the base case.

Table 3 showcases a comprehensive comparison of the suggested DO technique's performance with the findings of contemporary literatures, utilizing power loss reduction as a metric. The recommended technique presented results better than other techniques in every case that was examined.

#### 4.2. IEEE 69-Bus RDN

With total active power demand and total reactive power needed by loads set at 3.800MW and 2.700 MVAR, respectively, the IEEE 69-Bus RDN is operated at 12.66kV. The RDNs' line and load data can be obtained from [43]. The 33-bus RDN has 73 branches, of which 68 are normally closed branches (NCB) and 5 are normally opened branches (NOB). The branches [69 70 71 72 73] contain to the initial tie switches. The total active power loss, reactive power loss, VPI and AVSI in the base case results obtained after load flow are 224.99kW, 102.16kVAR, 1.5866 p.u, 0.9062 p.u, respectively. Fig. 7 showcases the line diagram of the IEEE 69-bus RDN. The outcomes for each scenario that the DO optimizer returned for its cost-based objective function are displayed in Table 4.

The new open branches acquired in scenario 2 (after NR alone) are [73 58 60 71 69], the configuration of these branches provided much lower real and reactive power losses, measuring 58.82 kW and 37.95 kVAR, respectively. The actual power loss is equivalent to a 73.86% decrease from the base case value of 224.99 kW prior to system modifications. At bus 27, the lowest voltage magnitude in p.u. was found to be 0.9712, with corresponding VPI and AVSI values of 2.1674 and 0.9627. The reconfiguration process resulted in the switching cost and the total cost benefit of 30 357.30(\$/npy) and 1 010 300.87(\$/npy).

For scenario 3 (SCA only), the algorithm returned shunt capacitors sizes (kVAR) of 878,204 and 179 situated at buses 61,64 and 21 respectively, with a reduced active and reactive power losses of 134.32kW and 94.28kVAR which corresponds to a 33.62% and 31.82% diminution in the active and reactive power losses, respectively in

relation to the base case. The obtained value for the minimum voltage magnitude, VPI and AVSI in p.u were 0.9283 at bus 65, 1.6530 and 0.9222, respectively. Finally, the total cost benefit incurred and Shunt Capacitor cost by the Shunt capacitor allocation were obtained to be 473 641.32(\$/npy) and 12 403.20(\$/npy), respectively.

Moving on to simulations in scenario 4 (simultaneous NR and SCA), It was found that the shunt capacitor sizes in kVAR are 150, 150, and 150 at buses 21, 6, and 59, respectively, and the new open branches obtained are [45,11,10,23 60]. It was discovered that the real and reactive power losses were 43.8 kW and 35.22 kVAR, respectively. This translates to reductions of 80.51 % in active power loss and 65.52% in reactive power loss when compared to the base scenario. The lowest voltage magnitude in p.u. was 0.9899 at bus 59, and the corresponding values for VPI and AVSI were 2.4680 and 0.9874. In conclusion, the synchronized reconfiguration of the RDN and shunt capacitors integrations resulted in total cost-benefit, switch cost, and shunt capacitor cost calculations of 1 134 722.596(\$/npy), 30 357.30(\$/npy), and \$4 426.20(\$/npy), respectively. Figs. 8, 9, 10, and 11 explain diagrammatically the notable improvements obtained on the RDN for all cases considered in terms of active power loss reduction, voltage profile enhancement, convergence characteristics, and the total reductions in operating costs, respectively when compared to the base case,

Table 5 showcases a comprehensive comparison of the suggested DO technique's performance with the findings of contemporary literature, utilizing power loss reduction as a metric. The recommended technique presented results better than other techniques in every case that was examined.

## 5. Conclusion

A novel optimizer (DO) and objective function has been effectively applied to simultaneously reconfigure RDN and allot shunt capacitors. The objective of the approach was to maximize the total cost benefits obtained from the decrease in the cost of energy procured from the DisCos through reduced power losses in radial distribution networks. While costs are never constant through time, the benefits obtained were scaled over a certain number of planning periods, considering interest and inflation rates in the modeling. Other technical benefits, such as AVSI and VPI, were also assessed. The suggested technique was validated on the IEEE 33-bus and 69-bus RDNs under various scenarios of reconfiguration, SC installation, synchronous reconfiguration, and SC integration. The simulation results revealed that making the cost-benefit

**Table 5**  
Comparison with Other Techniques for IEEE 69-Bus RDN.

Technique	Open branches	SC (kVAr)/ bus	Power loss (kW)	% Power loss reduction	Min. Bus Voltage (p.u)
Base case	69 70 71 72 73		224.99		0.9092
Scenario 2: Reconfiguration only					
COA [28]	69 70 14 57 61		98.59	56.18	0.9495
ICSA [44]	14 57 61 69 70		98.59	56.18	0.9495
HSA [28]	69 18 13 56 61		99.35	55.84	0.9428
FWA [28]	69 70 14 56 61		98.59	56.18	0.9495
ACSA [45]	69 70 14 57 61		98.59	56.18	0.9495
HM [46]	14 55 64 69 70		98.60	56.18	0.9428
UVDA [28]	14 58 61 69 70		98.58	56.18	0.9495
INNA [47]	14 57 61 69 70		98.60	56.18	0.9495
SFS [48]	14 55 61 69 70		98.62	56.17	0.9495
GWO[28]	69 14 71 61 58		98.63	56.16	0.9492
DO	73 58 60 71 69		58.82	73.86	0.9712
Scenario 3: SCA only					
AWOA [25]	69 70 71 72 73	150 (49) 150 (50) 1050 (61)	144.00	35.53	N.A.
LS [25]	69 70 71 72 73	350 (17) 1200 (16)	146.61	34.83	N.A.
GSA [25]	69 70 71 72 73	150 (26) 150 (13) 1050 (15)	145.90	35.14	N.A.
MFO [50]	69 70 71 72 73	300 (17) 1350(61)	145.69	35.24	N.A.
GWO [28]	69 70 71 72 73	697 (8) 260 (18) 1200 (60)	145.56	35.30	0.9319
WCA [28]	69 70 71 72 73	1288.20 (61) 213.40 (69) 270 (18)	144.53	35.76	0.9500
DO	69 70 71 72 73	878 (61) 204 (64) 179 (21)	144.36	35.83	0.9283
Scenario 4: Simultaneous reconfiguration and SCA					
GWO [28]	69 12 17 61 55	990 (12) 443 (49) 377 (10)	68.92	69.37	0.9660
MBBO [49]	10 19 14 60 54	600 (59) 300 (68) 300 (20)	80.61	64.16	N.A.
CS [49]	49 10 59 45 19	450 (8) 600 (30) 900 (23)	80.43	64.28	N.A.
MIC [25]	70 58 49 69 54	1350 (59) 150 (69) 450 (15)	102.85	54.28	N.A.

**Table 5 (continued)**

Technique	Open branches	SC (kVAr)/ bus	Power loss (kW)	% Power loss reduction	Min. Bus Voltage (p.u)
AWOA [25]	69 13 71 72 73	150 (49) 125 (50) 138 (61)	83.36	62.28	N.A.
DO	45 11 10 23 60	150 (21) 150 (6) 150 (59)	43.80	80.51	0.9728

the sole objective of the optimization process brought about significant power loss reduction compared to other objective functions utilized in the previously reviewed literature, with the algorithm returning a maximum of 69.2% active power loss reduction for the IEEE 33-bus RDN, and an improved 80.51% active power loss reduction for the IEEE 69-bus RDN, thereby, further establishing the efficacy of this approach. Future research could explore the application of this approach on an unbalanced distribution network. This approach could also be extended to the optimal allocation of electric vehicle charging stations (EVCS), FACTS (Flexible AC Transmission system) devices, and distributed generation (DG) in various distribution networks.

**CRedit authorship contribution statement**

**Ifeoluwa Olajide Fajinmi:** Writing – original draft, Methodology, Conceptualization. **Gafari Abiola Adepoju:** Writing – original draft, Investigation, Conceptualization. **Sunday Adeleke Salimon:** Validation, Methodology, Data curation. **Kareem M. AboRas:** Validation, Investigation, Formal analysis. **Oluwaseyi Wasiu Adebisi:** Software, Resources, Formal analysis. **Olunmi Onatoyinbo:** Writing – review & editing, Software, Investigation. **Mohammad Khishe:** Writing – review & editing, Visualization, Data curation. **Pradeep Jangir:** Writing – review & editing, Supervision, Conceptualization. **Wulfran Fendzi Mbasso:** Writing – review & editing, Supervision, Project administration.

**Declaration of competing interest**

The authors declare that they have no known competing financial interests or personal relationships that could have appeared to influence the work reported in this paper.

**Data availability**

Data will be made available on request.

**References**

- [1] P.K. Roy, S. Sultana, Optimal reconfiguration of capacitor based radial distribution system using chaotic quasi oppositional chemical reaction optimization, *Microsyst. Techn.* 28 (2) (2020) 499–511, <https://doi.org/10.1007/S00542-020-04885-8/METRICS>.
- [2] S. Wang, T. Lu, R. Hao, F. Wang, T. Ding, J. Li, X. He, Y. Guo, X. Han, An identification method for anomaly types of active distribution network based on data mining, *IEEE Trans. Power Syst.* (2023), <https://doi.org/10.1109/TPWRS.2023.3288043>.
- [3] J.D. Combata-Murcia, C.A. Romero-Salcedo, O.D. Montoya, D.A. Giral-Ramírez, Dynamic compensation of active and reactive power in distribution systems through PV-STATCOM and metaheuristic optimization, *Results. Eng.* 22 (2024) 102195, <https://doi.org/10.1016/J.RINENG.2024.102195>.
- [4] Sallam AA, Malik OP. *Electric Distribution System Modeling*. Piscataway, NJ: IEEE press; 2011.
- [5] O.D. Montoya, W. Gil-González, L.F. Grisales-Noreña, Optimal planning of photovoltaic and distribution static compensators in medium-voltage networks via the GND0 approach, *Results. Eng.* 23 (2024) 102764, <https://doi.org/10.1016/J.RINENG.2024.102764>.
- [6] RS Rao, SVL Narasimham, M. Ramalingaraju, Optimal capacitor placement in a radial distribution system using plant growth simulation algorithm, *Int. J. Electric. Power Energy Syst.* 33 (5) (2011) 1133–1139.

- [7] X. Chen, P. Yang, Y. Peng, M. Wang, F. Hu, J. Xu, Output voltage drop and input current ripple suppression for the pulse load power supply using virtual multiple quasi-notch-filters impedance, *IEEE Trans. Power. Electron.* 38 (8) (2023) 9552–9565, <https://doi.org/10.1109/TPEL.2023.3275304>.
- [8] J. Li, T. Lu, X. Yi, R. Hao, Q. Ai, Y. Guo, M. An, S. Wang, X. He, Y. Li, Concentrated solar power for a reliable expansion of energy systems with high renewable penetration considering seasonal balance, *Renew. Energy* 226 (2024) 120089, <https://doi.org/10.1016/J.RENENE.2024.120089>.
- [9] Adeyemo, I.A., Akinrogunde, O.O., & Salimon, S.A. (2022). Adaptive particle swarm optimization approach to simultaneous reconfiguration and shunt capacitor allocation in radial distribution network.
- [10] J. Li, T. Lu, X. Yi, M. An, R. Hao, Energy systems capacity planning under high renewable penetration considering concentrating solar power, *Sustain. Energy Techn. Assess.* 64 (2024) 103671, <https://doi.org/10.1016/J.SETA.2024.103671>.
- [11] M. Sedighzadeh, M. Dakhem, M. Sarvi, H.H. Kordkheili, Optimal reconfiguration and capacitor placement for power loss reduction of distribution system using improved binary particle swarm optimization, *Int. J. Energy Environ. Eng.* 5 (1) (2014) 1–11, <https://doi.org/10.1007/s40095-014-0073-9>.
- [12] P. Ushashree, K.S. Kumar, Power system reconfiguration in distribution system for loss minimization using optimization techniques: A review, *Wirel. Pers. Commun.* 128 (3) (2023) 1907–1940.
- [13] Mohamed El-Saeed, M.A.E. sayed, A.F. Abdel-Gwaad, M.A.E.fattah Farahat, Solving the capacitor placement problem in radial distribution networks, *Results. Eng.* 17 (2023) 100870, <https://doi.org/10.1016/J.RINENG.2022.100870>.
- [14] O.D. Montoya, A. Molina-Cabrera, D.A. Giral-Ramírez, E. Rivas-Trujillo, J. A. Alarcón-Villamil, Optimal integration of D-STATCOM in distribution grids for annual operating costs reduction via the discrete version sine-cosine algorithm, *Results. Eng.* 16 (2022) 100768, <https://doi.org/10.1016/J.RINENG.2022.100768>.
- [15] W. Xinyu, L. Haoran, K. Khan, Innovation in technology: a game changer for renewable energy in the European Union? *Nat. Resour. Forum.* (2024) <https://doi.org/10.1111/1477-8947.12450>.
- [16] E.A. Almasout, R.A. El-Sehiemy, O.N.U. An, O. Bayat, A hybrid local search-genetic algorithm for simultaneous placement of DG units and shunt capacitors in radial distribution systems, *IEEE Access.* 8 (2020) 54465–54481, <https://doi.org/10.1109/ACCESS.2020.2981406>.
- [17] S. Sadeghi, A. Jahangiri, A. Ghaderi Shamim, Optimal reconfiguration of a smart distribution network in the presence of shunt capacitors, *Electric. Eng.* 106 (1) (2023) 603–614, <https://doi.org/10.1007/S00202-023-01997-Y/METRICS>.
- [18] M.M. Sayed, M.Y. Mahdy, S.H.E. Abdel Aleem, H.K.M. Youssef, T.A. Boghdady, Simultaneous distribution network reconfiguration and optimal allocation of renewable-based distributed generators and shunt capacitors under uncertain conditions, *Energies* 2022 15 (6) (2022) 2299, <https://doi.org/10.3390/EN15062299>. Vol. 15, Page 2299.
- [19] H. Lotfi, Multi-objective network reconfiguration and allocation of capacitor units in Radial distribution system using an enhanced artificial bee colony optimization, *Electric Power Compon. Syst.* 49 (13–14) (2022) 1130–1142, <https://doi.org/10.1080/15325008.2022.2049661>.
- [20] Y. Gebru, D. Bitew, H. Aberie, K. Gizaw, Performance enhancement of radial distribution system using simultaneous network reconfiguration and switched capacitor bank placement, *Cogent. Eng.* 8 (1) (2021), <https://doi.org/10.1080/23311916.2021.1897929>.
- [21] S.R. Biswal, G. Shankar, R.M. Elavarasan, L. Mihet-Popa, Optimal allocation/sizing of DG/capacitors in reconfigured radial distribution system using quasi-reflected slime mould algorithm, *IEEE Access.* 9 (2021) 125658–125677, <https://doi.org/10.1109/ACCESS.2021.3111027>.
- [22] L.A. Gallego, J.M. Lopez-Lezama, O.G. Carmona, A mixed-integer linear programming model for simultaneous optimal reconfiguration and optimal placement of capacitor banks in distribution networks, *IEEE Access.* 10 (2022) 52655–52673, <https://doi.org/10.1109/ACCESS.2022.3175189>.
- [23] M. Beirami, S. Naghdalian, M.H. Aliabadi, Probabilistic multiobjective reconfiguration considering the optimal location of shunt capacitors and distributed generations in distribution network, *Int. Trans. Electric. Energy Syst.* 31 (9) (2021) e12979, <https://doi.org/10.1002/2050-7038.12979>.
- [24] A. Shaheen, A. Elsayed, A. Ginidi, R. El-Sehiemy, E. Elattar, Reconfiguration of electrical distribution network-based DG and capacitors allocations using artificial ecosystem optimizer: practical case study, *Alexandria Eng. J.* 61 (8) (2022) 6105–6118, <https://doi.org/10.1016/J.AEJ.2021.11.035>.
- [25] M.R. Babu, C.V. Kumar, S. Anitha, Simultaneous reconfiguration and optimal capacitor placement using adaptive whale optimization algorithm for radial distribution system, *J. Electric. Eng. Techn.* 16 (1) (2021) 181–190, <https://doi.org/10.1007/S42835-020-00593-5/METRICS>.
- [26] E. Mohamed, A.A.A. Mohamed, Y. Mitani, MSA for optimal reconfiguration and capacitor allocation in radial/ring distribution networks, *Int. J. Interact. Multimedia Artific. Intellig.* 5 (1) (2018) 107, <https://doi.org/10.9781/IJIMAI.2018.05.002>.
- [27] M. Abd-El-, H. Mohamed, Z.M. Ali, M. Ahmed, S.F. Al-Gahtani, C. Mohamed, -E. H. Ali, Z.M. Ahmed, M. Al-Gahtani, Energy saving maximization of balanced and unbalanced distribution power systems via network reconfiguration and optimum capacitor allocation using a hybrid metaheuristic algorithm, *Energies.* 14 (11) (2021) 3205, <https://doi.org/10.3390/EN14113205>, 2021, Vol. 14, Page 3205.
- [28] T. Jayabarathi, A. Raghunathan, T. Mithulananthan, N. Cherukuri, S.H. C. G.L Sai, Enhancement of distribution system performance with reconfiguration, *Distribut. Gener. Capacitor Bank Deploym.* (2024), <https://doi.org/10.1016/j.heliyon.2024.e26343>.
- [29] P.S. Prasad, M. Sushama, Distribution network reconfiguration and capacitor allocation in Distribution system using discrete improved Grey wolf optimization, *Lect. Notes Electric. Eng.*, 894 LNEE (2022) 602–617, [https://doi.org/10.1007/978-981-19-1677-9\\_54/COVER](https://doi.org/10.1007/978-981-19-1677-9_54/COVER).
- [30] B. Stojanović, T. Rajić, D. Sošić, Distribution network reconfiguration and reactive power compensation using a hybrid Simulated Annealing – Minimum spanning tree algorithm, *Int. J. Electric. Power Energy Syst.* 147 (2023) 108829, <https://doi.org/10.1016/J.IJEPES.2022.108829>.
- [31] A.A.El Desouky, A.A. Eldesouky, E.M. Reyad, G.A Mahmoud, Implementation of boolean PSO for service restoration using distribution network reconfiguration simultaneously with distributed energy resources and capacitor banks, *Article Intern. J. Ren. Energy Res.* 10 (1) (2020). <https://www.researchgate.net/publication/352156774>.
- [32] M. Mahdavi, H.H. Alhelou, M.R. Hesamzadeh, An efficient stochastic reconfiguration model for distribution systems with uncertain loads, *IEEE Access.* 10 (2022) 10640–10652, <https://doi.org/10.1109/ACCESS.2022.3144665>.
- [33] O. Kahouli, H. Alsaif, Y. Bouteraa, N. Ben Ali, M. Chaabene, Power system reconfiguration in distribution network for improving reliability using genetic algorithm and particle swarm optimization, *Appl. Sci.* 11 (7) (2021) 3092, <https://doi.org/10.3390/AP11073092>, 2021, Vol. 11, Page 3092.
- [34] S. Mehroliya, A. Arya, Distributed generator and capacitor-embedded reconfiguration in three-phase unbalanced distribution systems using teaching learning-based optimization, *Comput. Applic. Eng. Educ.* 32 (1) (2024) e22689, <https://doi.org/10.1002/CAE.22689>.
- [35] S Nagaballi, VS. Kale, A metaphor-less based AI technique for optimal deployment of DG and DSTATCOM considering reconfiguration in the RDS for techno-economic benefits, *J. Intellig Fuzzy Syst.* 41 (5) (2021) 5719–5729.
- [36] R Arulraj, N. Kumarappan, Optimal economic-driven planning of multiple DG and capacitor in distribution network considering different compensation coefficients in feeder's failure rate evaluation, *Engineering Science and Technology, an, Intern. J.* 22 (1) (2019) 67–77.
- [37] GA Adepoju, SA Salimon, IG Adebayo, OB. Adewuyi, Impact of DSTATCOM penetration level on technical benefits in Radial distribution network. *E-prime-advances in electrical engineering, Electr. Energy* (2023) 100413.
- [38] SA Salimon, GA Adepoju, IG Adebayo, SO. Ayanlade, Impact of shunt capacitor penetration level in radial distribution system considering techno-economic benefits, *Nigerian J. Technologic. Developm.* 19 (2) (2022) 101–109.
- [39] S. Zhao, T. Zhang, S. Ma, M. Chen, Dandelion optimizer: A nature-inspired metaheuristic algorithm for engineering applications, *Eng. Appl. Artif. Intell.* 114 (2022) 105075, <https://doi.org/10.1016/J.ENGAPPAI.2022.105075>.
- [40] M Mohammadi, AM Rozbahani, S. Bahmanyar, Power loss reduction of distribution systems using BFO based optimal reconfiguration along with DG and shunt capacitor placement simultaneously in fuzzy framework, *J. Cent. South. Univ.* 24 (1) (2017) 90–103.
- [41] J.H. Teng, A direct approach for distribution system load flow solutions, *IEEE Trans. Power Deliv.* 18 (3) (2003) 882–887, <https://doi.org/10.1109/TPWRD.2003.813818>.
- [42] D.B. Santos, S. Sarjiya, F.P. Sakti, Optimal sizing and placement of wind-based distributed generation to minimize losses using flower pollination algorithm, *JTERA (Jurnal Teknologi Rekayasa)* 3 (2) (2018) 167, <https://doi.org/10.31544/jtera.v3.i2.2018.167-176>.
- [43] A.F. Abdul kadir, A. Mohamed, H. Shareef, M.Z. Che Wanik, Optimal placement and sizing of distributed generations in distribution systems for minimizing losses and THDv using evolutionary programming, *Turkish J. Electric. Eng. Comput. Sci.* 21 (SUPPL. 2) (2013) 2269–2282, <https://doi.org/10.3906/elk-1205-35>.
- [44] T.T. Nguyen, T.T. Nguyen, An improved cuckoo search algorithm for the problem of electric distribution network reconfiguration, *Appl. Soft. Comput.* 84 (2019) 105720, <https://doi.org/10.1016/J.ASOC.2019.105720>.
- [45] T.T. Nguyen, A.V. Truong, T.A. Phung, A novel method based on adaptive cuckoo search for optimal network reconfiguration and distributed generation allocation in distribution network, *Int. J. Electric. Power Energy Syst.* 78 (2016) 801–815, <https://doi.org/10.1016/J.IJEPES.2015.12.030>.
- [46] K. Jasthi, D. Das, Simultaneous distribution system reconfiguration and DG sizing algorithm without load flow solution, *IET Generat., Transm. Distrib.* 12 (6) (2018) 1303–1313, <https://doi.org/10.1049/IET-GTD.2017.033>.
- [47] T.Van Tran, B.H. Truong, T.P. Nguyen, T.A. Nguyen, T.L. Duong, D.N Vo, Reconfiguration of distribution networks with distributed generations using an improved neural network algorithm, *IEEE Access.* 9 (2021) 165618–165647, <https://doi.org/10.1109/ACCESS.2021.3134872>.
- [48] T.T. Tran, K.H. Truong, D.N. Vo, Stochastic fractal search algorithm for reconfiguration of distribution networks with distributed generations, *Ain Shams Eng. J.* 11 (2) (2020) 389–407, <https://doi.org/10.1016/J.ASEJ.2019.08.015>.
- [49] A.N. Hussain, W.K. Shakir Al-Jubori, H.F. Kadom, Hybrid design of optimal capacitor placement and reconfiguration for performance improvement in a radial distribution system, *J. Eng. (United Kingdom)* 2019 (2019), <https://doi.org/10.1155/2019/1696347>.
- [50] A.A.Z. Diab, H. Rezk, Optimal sizing and placement of capacitors in radial distribution systems based on Grey Wolf, Dragonfly and Moth-Flame optimization algorithms, *Iranian J.Sci. Techn. - Transact. Electric. Eng.* 43 (1) (2019) 77–96, <https://doi.org/10.1007/S40998-018-0071-7/METRICS>.